Inorganic Chemistry
Article

Inorg. Chem. **2009**, *48*, 6845–6851 **6845**
DOI: 10.1021/ic9007735

Homometallic Uranium(VI) Phosphonoacetates Containing Interlayer Dipyridines

Karah E. Knope and Christopher L. Cahill*

Department of Chemistry, The George Washington University, 725 21st Street NW, Washington, D.C. 20052

Received April 21, 2009

Three organically templated uranium(VI) carboxyphosphonates, $[C_{10}H_{10}N_2][(UO_2)_3(PPA)_2(HPPA)(H_2O)]\cdot 3H_2O$ **(1)**, $[C_{12}H_{12}N_2][(UO_2)_3(PPA)_2(HPPA)(H_2O)]\cdot 2H_2O$ **(2)**, and $[C_{12}H_{14}N_2][(UO_2)_3(PPA)_2(HPPA)(H_2O)]\cdot 2H_2O$ **(3)** have been prepared from hydrothermal reactions of $UO_2(NO_3)_2\cdot 6H_2O$ and phosphonoacetic acid ($H_2O_3PCH_2CO_2H$, H_3PPA) in the presence of 4,4′-dipyridyl, 1,2-bis(4-pyridyl)-ethylene and 1,2-bis(4-pyridyl)-ethane. The crystal structures of **1**−**3** are built from UO_7 units linked via phosphonoacetate molecules to form 2-dimensional $[(UO_2)_3(PPA)_2(HPPA)(H_2O)]^{2-}$ networks which are charge balanced by doubly protonated bipyridyl molecules. Interaction of the pyridyl molecules with other functionalities present in **1**−**3** result in relatively strong N−H···O (2.707−3.155 Å) and weaker C−H···O (2.948−3.237 Å) interactions that constitute the interlayer. Water-carboxylate O−H···O hydrogen bonding (2.548−2.675 Å) in **1**−**3** and $\pi-\pi$ interactions (3.708 Å) between pyridyl rings in **2** also exist in these materials. Reported herein are the syntheses, structural characterization, and thermal and fluorescent behavior of **1**−**3**.

Introduction

Uranium(VI) solid-state structures assembled from mono- and multifunctional phosphonates display a variety of structural features and topologies, adopting chain, layered, tubular and 3-dimensional architectures.[1−9] In addition to the rich structural chemistry presented by these materials, interesting luminescent properties and phase transitions such as those found in UO_2^{2+}/phenylphosphonate systems[3,4] have also been reported. To this end, the syntheses, crystal chemistry, and properties of U(VI) phosphonates containing structure directing agents[6] and more recently bi- and/or heterofunctional phosphonates have been explored.[7,9,10] From a structural perspective, the use of multifunctional linkers within U(VI) containing coordination polymer (CP) and metal organic framework (MOF) syntheses, more generally, has been quite successful.[11−20] This is perhaps best illustrated by the diverse family of hybrid UO_2^{2+}-organic architectures assembled from dicarboxylate ligands.[21−34] Uranyl containing materials also exhibit interesting

*To whom correspondence should be addressed. E-mail: cahill@gwu.edu.

(1) Clearfield, A. In *Progress in Inorganic Chemistry*; Karlin, K. D., Ed.; John Wiley & Sons: New York, 1998; Vol. *47*, p 371−510.
(2) Grohol, D.; Subramanian, M. A.; Poojary, D. M.; Clearfield, A. *Inorg. Chem.* **1996**, *35*, 5264–5271.
(3) Grohol, D.; Clearfield, A. *J. Am. Chem. Soc.* **1997**, *119*, 4662–4668.
(4) Grohol, D.; Clearfield, A. *J. Am. Chem. Soc.* **1997**, *119*, 9301–9302.
(5) Grohol, D.; Gingl, F.; Clearfield, A. *Inorg. Chem.* **1999**, *38*, 751–756.
(6) Doran, M. B.; Norquist, A. J.; O'Hare, D. *Chem. Mater.* **2003**, *15*, 1449–1455.
(7) Alsobrook, A. N.; Zhan, W.; Albrecht-Schmitt, T. E. *Inorg. Chem.* **2008**, *47*, 5177–5183.
(8) Bao, S.-S.; Chen, G.-S.; Wang, Y.; Li, Y.-Z.; Zheng, L.-M.; Luo, Q.-H. *Inorg. Chem.* **2006**, *45*, 1124–1129.
(9) Nelson, A.-G. D.; Bray, T. H.; Zhan, W.; Haire, R. G.; Sayler, T. S.; Albrecht-Schmitt, T. E. *Inorg. Chem.* **2008**, *47*, 4945–4951.
(10) Knope, K. E.; Cahill, C. L. *Inorg. Chem.* **2008**, *47*, 7660–7672.
(11) Cahill, C. L.; Borkowski, L. A. In *Structural Chemistry of Inorganic Actinide Compounds*; Krivovichev, S. V., Burns, P. C., Tananaev, I. G., Eds.; Elsevier: Amsterdam, 2007, p 419.
(12) Cahill, C. L.; de Lill, D. T.; Frisch, M. *CrystEngComm* **2007**, *9*, 15–26.
(13) Kim, J.-Y.; Norquist, A. J.; O'Hare, D. *Chem. Mater.* **2003**, *15*, 1970–1975.
(14) Thuery, P. *Chem. Commun.* **2006**, 853–855.
(15) Thuery, P. *Inorg. Chem.* **2007**, *46*, 2307–2315.
(16) Thuery, P. *Inorg. Chem. Commun.* **2007**, *10*, 423–426.
(17) Xie, Y.-r.; Zhao, H.; Wang, X.-s.; Qu, Z.-r.; Xiong, R.-g.; Xue, X.; Xue, Z.; You, X.-z. *Eur. J. Inorg. Chem.* **2003**, 3712–3715.
(18) Thuery, P. *Cryst. Growth Des.* **2008**, *8*, 4132–4143.
(19) Thuery, P. *Cryst. Growth Des.* **2009**, *9*, 1208–1215.
(20) Thuery, P.; Masci, B. *Cryst. Growth Des.* **2008**, *8*, 3430–3436.
(21) Borkowski, L. A.; Cahill, C. L. *Inorg. Chem.* **2003**, *42*, 7041–7045.
(22) Borkowski, L. A.; Cahill, C. L. *Cryst. Growth Des.* **2006**, *6*, 2241–2247.
(23) Borkowski, L. A.; Cahill, C. L. *Cryst. Growth Des.* **2006**, *6*, 2248–2259.
(24) Frisch, M.; Cahill, C. L. *Dalton Trans.* **2005**, 1518–1523.
(25) Frisch, M.; Cahill, C. L. *Dalton Trans.* **2006**, 4679–4690.
(26) Frisch, M.; Cahill, C. L. *J. Solid State Chem.* **2007**, *180*, 2597–2602.
(27) Dean, N. E.; Hancock, R. D.; Cahill, C. L.; Frisch, M. *Inorg. Chem.* **2008**, *47*, 2000–2010.
(28) Thuery, P. *Polyhedron* **2007**, *26*, 101–106.
(29) Thuery, P. *CrystEngComm* **2009**, *11*, 232–234.
(30) Masci, B.; Thuery, P. *CrystEngComm* **2008**, *10*, 1082–1087.
(31) Kim, J.-Y.; Norquist, A. J.; O'Hare, D. *Dalton Trans.* **2003**, 2813–2814.
(32) Duvieubourg, L.; Nowogrocki, G.; Abraham, F.; Grandjean, S. *J. Solid State Chem.* **2005**, *178*, 3437–3444.
(33) Zheng, Y.-Z.; Tong, M.-L.; Chen, X.-M. *Eur. J. Inorg. Chem.* **2005**, 4109–4117.
(34) Thuery, P. *CrystEngComm* **2008**, *10*, 1126–1128.

Published on Web 06/22/2009

Table 1. Crystallographic Data and Structure Refinement for **1**−**3**

	1	**2**	**3**
empirical formula	$C_{16}H_{25}N_2O_{25}P_3U_3$	$C_{18}H_{25}N_2O_{24}P_3U_3$	$C_{18}H_{27}N_2O_{24}P_3U_3$
fw	1452.38	1460.40	1462.42
temp (K)	295(2)	295(2)	295(2)
λ (Mo Kα)	0.71073	0.71073	0.71073
crystal system	monoclinic	triclinic	triclinic
space group	$P2_1/c$	$P\bar{1}$	$P\bar{1}$
a (Å)	8.9801(4)	10.5063(4)	10.4115(5)
b (Å)	25.5577(11)	10.8858(4)	10.9064(5)
c (Å)	13.8436(6)	15.6464(6)	15.7534(8)
α (deg)	90	105.564(1)	105.895(1)
β (deg)	100.313(1)	95.246(1)	95.653(1)
γ (deg)	90	104.024(1)	103.470(1)
V (Å^3)	3125.9(2)	1648.87(11)	1647.73(14)
Z	4	2	2
D_{calc} (g·cm^{-3})	3.086	2.941	2.948
μ (mm^{-1})	15.763	14.940	14.951
R_{int}	0.0514	0.0935	0.0752
R_1[a] $[I > 2\sigma(I)]$	0.0275	0.0339	0.0299
wR_2[a]	0.0543	0.0836	0.0579

[a] $R_1 = \sum||F_o| - |F_c||/\sum|F_o|$; $wR_2 = \{\sum w(F_o^2 - F_c^2)^2/\sum w(F_o^2)^2\}^{1/2}$.

photoluminescent properties and photocatalytic activity.[12,35−42] The unique structural chemistry and remarkable physiochemical properties of the UO_2^{2+} cation thus provide much impetus for the synthesis and characterization of novel U(VI) containing materials.

We recently reported the synthesis, crystal structures, thermal and fluorescent behavior of several homometallic U(VI) carboxyphosphonates.[10] These materials exhibit a range of structural motifs and topologies resulting from variations in metal−ligand coordination modes, P−C−C−O torsion angles, and interlayer hydrogen bonding networks. Moreover, synthetic variables such as in situ ligand formation, the addition of nominally "spectator" species, and the incorporation of charge balancing countercations were found to influence product formation. As an extension of the latter, we have presently explored hydrothermal reactions of uranium oxynitrate and phosphonoacetic acid in the presence of organic dipyridyls (4,4′-dipyridyl, 1,2-bis(4-pyridyl)-ethylene, and 1,2-bis(4-pyridyl)-ethane). Reported herein are the syntheses, structural characterization, and thermal and fluorescent behavior of three novel templated uranium(VI) phosphonoacetates, $[C_{10}H_{10}N_2][(UO_2)_3(PPA)_2(HPPA)(H_2O)]\cdot 3H_2O$ **(1)**, $[C_{12}H_{12}N_2][(UO_2)_3(PPA)_2(HPPA)(H_2O)]\cdot 2H_2O$ **(2)**, and $[C_{12}H_{14}N_2][(UO_2)_3(PPA)_2(HPPA)(H_2O)]\cdot 2H_2O$ **(3)**.

Experimental Section

Synthesis. ***Caution!*** *Whereas the uranium oxynitrate* $(UO_2)(NO_3)_2\cdot 6H_2O$ *used in this investigation contains depleted U, standard precautions for handling radioactive substances should be followed.*

Compounds **1**−**3** were synthesized hydrothermally. **(1)** Uranium oxynitrate hexahydrate (0.174 g, 0.35 mmol), phosphonoacetic acid (0.101 g, 0.72 mmol), 4,4′-dipyridyl (0.055 g, 0.35 mmol), and distilled water (4 g, 224 mmol) were placed into a 23 mL Teflon-lined Parr bomb in the approximate molar ratios of 1:2:1:640 respectively. The reaction vessel was then sealed and heated statically in an isothermal oven at 150 °C. After 4 days, the reaction vessels were removed from the oven, placed on the benchtop, and cooled to room temperature over 4 h. The mother liquor was decanted and yellow crystals were obtained. The crystals were washed with distilled water, sonicated, and washed in ethanol and then allowed to air-dry at room temperature. Compounds **(2)** and **(3)** were prepared by replacing 4,4′-dipyridyl with 1,2-bis(4-pyridyl)-ethylene (bpe) and 1,2-bis(4-pyridyl)-ethane (bpa), respectively. Yield (based on uranium); elemental analysis (via combustion, Galbraith Laboratories, Knoxville, TN), observed (calculated): **(1)** 86%; C 13.09% (13.23%), H 1.62% (1.73%), N 1.86% (1.92%); **(2)** 88%; C 14.74% (14.80%), H 1.64% (1.73%), N 1.84% (1.92%); **(3)** 92%; C 14.58% (14.78%), H 1.70% (1.86%), N 1.79% (1.91%).

X-ray Structure Determination. A single crystal from each of the samples was isolated from the bulk and mounted on a glass fiber. Reflections were collected at room temperature on a Bruker SMART diffractometer equipped with an APEX II CCD detector using Mo Kα radiation and a combination of 0.5° ω and φ scans. The data were integrated and corrected for absorption using the APEX II suite of crystallographic software.[43,44] All compounds were solved using direct methods and refined using SHELXL-97[45] within the WinGX software suite.[46] Satisfactory refinements as well as tests for missing symmetry, using Platon,[47] indicated that no obvious space group changes were needed or suggested. Crystallographic data for **1**−**3** are provided in Table 1, and CIF data are available as Supporting Information. Crystallographic data have been deposited with the Cambridge Crystallographic Data Centre (CCDC) and may be obtained at http://www.ccdc.cam.ac.uk/ by citing reference nos. 728869−728871.

(35) Rabinowitch, E.; Belford, R. L. *Spectroscopy and Photochemistry of Uranyl Compounds*; MacMillan: New York, 1964.
(36) Burrows, H. D.; Kemp, T. J. *Chem. Soc. Rev.* **1974**, *3*, 139–65.
(37) Chen, W.; Yuan, H.-M.; Wang, J.-Y.; Liu, Z.-Y.; Xu, J.-J.; Yang, M.; Chen, J.-S. *J. Am. Chem. Soc.* **2003**, *125*, 9266–9267.
(38) Yu, Z.-T.; Liao, Z.-L.; Jiang, Y.-S.; Li, G.-H.; Chen, J.-S. *Chem.—Eur. J.* **2005**, *11*, 2642–2650.
(39) Jiang, Y.-S.; Yu, Z.-T.; Liao, Z.-L.; Li, G.-H.; Chen, J.-S. *Polyhedron* **2006**, *25*, 1359–1366.
(40) Mao, Y.; Bakac, A. *Inorg. Chem.* **1996**, *35*, 3925–3930.
(41) Harrowfield, J. M.; Lugan, N.; Shahverdizadeh, G. H.; Soudi, A. A.; Thuery, P. *Eur. J. Inorg. Chem.* **2006**, 389–396.
(42) Nieweg, J. A.; Lemma, K.; Trewyn, B. G.; Lin, V. S. Y.; Bakac, A. *Inorg. Chem.* **2005**, *44*, 5641–5648.
(43) *APEX II software suite*, v.2008.3-0; Bruker AXS: Madison, WI, 2008.
(44) Sheldrick, G. M. *SADABS*, v. 2008/1; University of Göttingen: Göttingen, Germany, 2008.
(45) Sheldrick, G. M. *Acta Crystallogr.* **2008**, *A64*, 112–122.
(46) Farrugia, L. J. *J. Appl. Crystallogr.* **1999**, *32*, 837–838.
(47) Spek, A. L. *Acta Crystallogr., Sect. A* **1990**, *46*, C34.

All non-hydrogen atoms were located using difference Fourier maps and were ultimately refined anisotropically. Hydrogen atoms of the phosphonacetate $-CH_2$ groups and pyridyl $-CH$ were placed in calculated positions, and bond distances were fixed at 0.97 Å and 0.93 Å, respectively. During the refinement of **1**, pyridyl N−H and −COOH hydrogen atoms were located in difference Fourier maps and refined freely. Although residual electron density attributed to pyridyl N−H hydrogen atoms was found in difference Fourier maps, assignments as such did not yield satisfactory refinements in **2**. Pyridyl hydrogen atoms were thus placed in calculated positions. Alternatively, hydrogen atoms residing on the nitrogen atoms of 1,2-bis(4-pyridyl)-ethane in **3** were located and refined with distance restraints of 0.89 Å. Hydrogen atoms of the lattice water molecules in **1**−**3** were not found during refinement, yet hydrogen atoms of the bound water molecules were located in difference Fourier maps. Hydrogen atoms of the bound water molecule in **1** were refined with distance restraints of 0.80 Å whereas those in **2** and **3** were refined freely.

Powder X-ray diffraction data were collected for **1**−**3** using a Rigaku Miniflex diffractometer (Cu Kα, 3−60°) and manipulated using the JADE software package.[48] Agreement between the calculated and observed patterns shown in Supporting Information, Figures SI 1−3 confirm that the single crystals used for structure determination were representative of the bulk sample.

Characterization. Thermogravimetric analysis (TGA) was performed on a Perkin-Elmer Pyris1 at a rate of 10 °C/min over a temperature range of 30−600 °C under flowing nitrogen gas. IR spectra were obtained on a Perkin-Elmer Spectrum RX1 FTIR system. The sample was diluted with spectroscopic KBr (dried) and pressed into a pellet. Scans were run over the range 4000−400 cm^{-1} with 8 scans and 2 cm^{-1} resolution. Emission spectra were collected on a Shimadzu RF-5301 PC Spectrofluorophotometer (uranium excitation wavelength 365 nm; emission wavelength: 450−600 nm; slit width: 1.5 nm (excitation) and 1.5 nm (emission); sensitivity: high with a UV-35 filter). All TGA plots, PXRD data, and IR spectra can be found in the Supporting Information.

Results

Structure Description. The crystal structures of **1**−**3** all consist of $(UO_2)O_5$ pentagonal bipyramidal building units. The composition of the $[(UO_2)_3(PPA)_2(HPPA)(H_2O)]^{2-}$ layers in **1**−**3** are equivalent; however, the topology of the anionic sheets in **1** is distinct from that found in **2** and **3**. Subtle topological differences between the two sheets result from slight variations in metal−ligand connectivity as illustrated by the coordination behavior of the P(2)PA ligands discussed below. The anionic sheets of **2** and **3** are structurally analogous and therefore the structure of **2** is described more fully and only a brief structural description of **3** is provided. Table 2 lists selected bond lengths and angles for **1**−**3**. ORTEP illustrations are included in the Supporting Information, Figures SI 4−6.

Compound **1**, $[C_{10}H_{10}N_2][(UO_2)_3(PPA)_2(HPPA)(H_2O)]\cdot 3H_2O$ (Figure 1), is built from three crystallographically distinct U(VI) metal centers and three unique phosphonoacetate ligands. Each U(VI) site is characteristically bound to two axial oxygen atoms [U1(O1, O2), U2(O11, O12), and U3(O13, O14)] to form the UO_2^{2+} cation, with an average U═O bond distance of 1.77 Å and an average O═U═O bond angle of 178.4°. Additionally each UO_2^{2+} is equatorially bound to five oxygen atoms, with U−O bond distances ranging from 2.284(4) Å to 2.593(4) Å, to result in pentagonal bipyramid geometry. U(1) is coordinated to four phosphonoacetic acid units. Two acid units, P(1)PA and P(2)PA, are coordinated through a single phosphonate oxygen (O4 and O5, respectively) with an average bond distance of 2.304 Å. A third phosphonoacetate molecule, P(3)PA, is bound in bidentate fashion through carboxylate oxygen atoms O6 and O7 at distances of 2.547(4) Å and 2.593(4) Å, respectively. The coordination environment of U(1) is

(48) *JADE*, V6.1; Materials Data Inc.: Livermore, CA, 2002.

Table 2. Selected Bond Distances (Å) and Angles (deg) for **1**−**3**

	Compound **1**[a]		
U(1)−O(1)	1.763(4)	P(1)−O(4)	1.518(4)
U(1)−O(2)	1.766(4)	P(1)−C(1)	1.811(7)
U(1)−O(4)	2.313(4)	C(1)−C(2)	1.497(9)
U(2)−O(11)	1.773(4)	O(21)−C(2)	1.198(8)
U(2)−O(12)	1.768(4)	O(22)−C(2)	1.310(9)
U(2)−O(10)	2.349(4)	O(7)−C(5)	1.253(6)
U(3)−O(13)	1.768(4)	C(5)−C(6)	1.509(7)
U(3)−O(14)	1.774(4)	C(40)−C(41)	1.363(9)
U(3)−O(16)^2	2.488(4)	N(1)−C(40)	1.331(9)
D−H···A	***d*(D···A)**	**Bond Angles**	
O(9)−H(9A)···O(19)^5	2.880(6)	O(2)−U(1)−O(1)	176.7(2)
O(9)−H(9B)···O(16)^1	2.663(6)	O(12)−U(2)−O(11)	179.3(2)
O(22)−H(22A)···OH(3)	2.563(9)	O(13)−U(3)−O(14)	179.2(2)
N(1)−HN(1)···O(7) ^{6}	2.773(7)		
N(2)−HN(2)···O(21)^1	2.814(8)		
	Compound **2**		
U(1)−O(6)	1.762(4)	P(1)−O(19)	1.512(4)
U(1)−O(3)	1.777(4)	P(1)−C(5)	1.831(6)
U(1)−O(7)	2.496(4)	C(5)−C(6)	1.525(10)
U(2)−O(1)	1.762(4)	O(22)−C(6)	1.323(9)
U(2)−O(2)	1.776(4)	O(20)−C(6)	1.207(10)
U(2)−O(16)	2.475(4)	N(31)−C(41)	1.331(10)
U(3)−O(9)	1.780(4)	C(31)−C(36)	1.357(9)
U(3)−O(4)	1.780(4)	C(33)−C(34)	1.469(9)
U(3)−O(8)	2.265(4)	C(32)−C(33)	1.318(9)
D−H···A	***d*(D···A)**	**Bond Angles**	
O(22)−H(22)···OW1^6	2.675(11)	O(6)−U(1)−O(3)	177.5(2)
N(30)−HN30···O(7)	2.707(7)	O(1)−U(2)−O(2)	178.9(2)
N(31)−HN31···O(20)^7	2.967(9)	O(9)−U(3)−O(4)	179.2(2)
N(31)−HN31···O(6)^7	3.155(8)		
O(16)−H(16A)···O(11)^2	2.665(6)		
	Compound **3**		
U(1)−O(13)	1.779(5)	P(1)−C(4)	1.809(8)
U(1)−O(11)	1.783(5)	C(5)−C(4)	1.533(12)
U(1)−O(12)	2.493(5)	C(5)−O(21)	1.194(10)
U(1)−O(10)	2.303(4)	C(5)−O(22)	1.327(10)
U(2)−O(15)	2.480(6)	N(21)−C(31)	1.291(13)
U(2)−O(14)	2.575(5)	C(25)−C(26)	1.325(14)
U(3)−O(14)^2	2.586(4)	C(31)−C(30)	1.347(14)
O(10)−P(1)	1.511(5)		
D−H···A	***d*(D···A)**	**Bond Angles**	
O(22)−H(22A)···OW1	2.669(11)	O(13)−U(1)−O(11)	177.5(2)
O(15)−H(15A)···O20	2.659(8)	O(9)−U(2)−O(8)	178.6(2)
O(15)−H(15B)···O5	3.014(8)	O(1)−U(3)−O(2)	178.7(2)
O(15)−H(15B)···O3	3.300(8)		
N(21)−HN(21)···O21	2.927(10)		
N(21)−HN(21)···O11	3.148(10)		
N(20)−HN(20)···O12	2.722(9)		

[a] Symmetry transformations: (**1**) 1, −*x*,−*y*,−*z* ; 2, *x*, −*y*+1/2, *z*+1/2 ; 3, −*x*, −*y*, −*z* + 1 ; 4, *x*, −*y*+1/2, *z* − 1/2 ; 5, −*x*, *y*−1/2, −*z*+1/2 ; 6, −*x*+1, −*y*, −*z*+1 (**2**) 2, −*x*+1,−*y*+2,−*z* ; 6, −*x*+2,−*y*+1,−*z*+1 ; 7, *x*, *y*+1,*z*+1. (**3**) 1, −*x*+1,−*y*+1,−*z*+2; 2, *x*,*y*−1,*z* ; 3, *x*,*y*+1,*z* ; 4, −*x*+1, −*y*,−*z*+2; 5, −*x*,−*y*+1,−*z*+1; 6 −*x*,−*y*,−*z*+1.

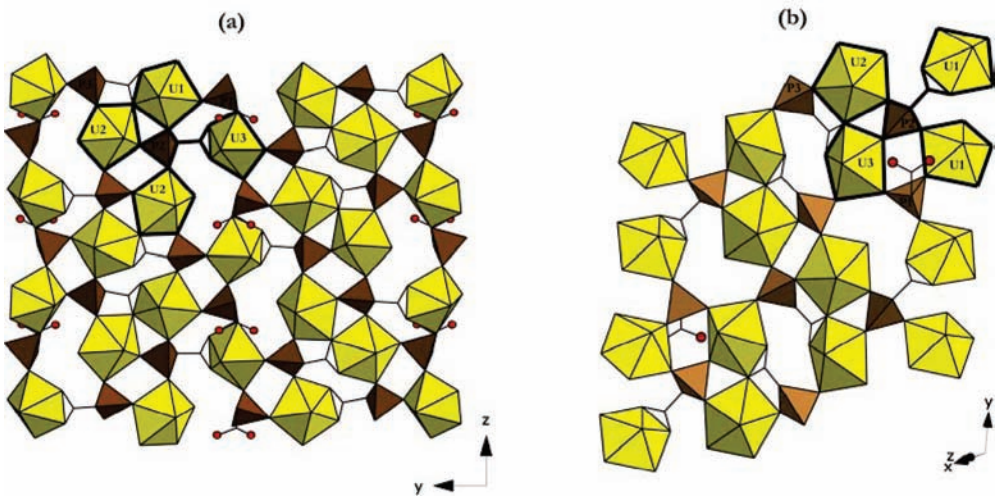

Figure 1. Polyhedral representation of **1** (a) and **2** (b) illustrating the topology of the 2-dimensional $[(UO_2)_3(PPA)_2(HPPA)(H_2O)]^{2-}$ networks built from UO_7 units linked via phosphonoacetate molecules. Yellow polyhedra are uranium(VI) atoms in pentagonal bipyramid geometry. Brown polyhedra and black lines represent the phosphorus and carbon atoms of the phosphonoacetate ligand. Heavy lines highlight local coordination discussed below.

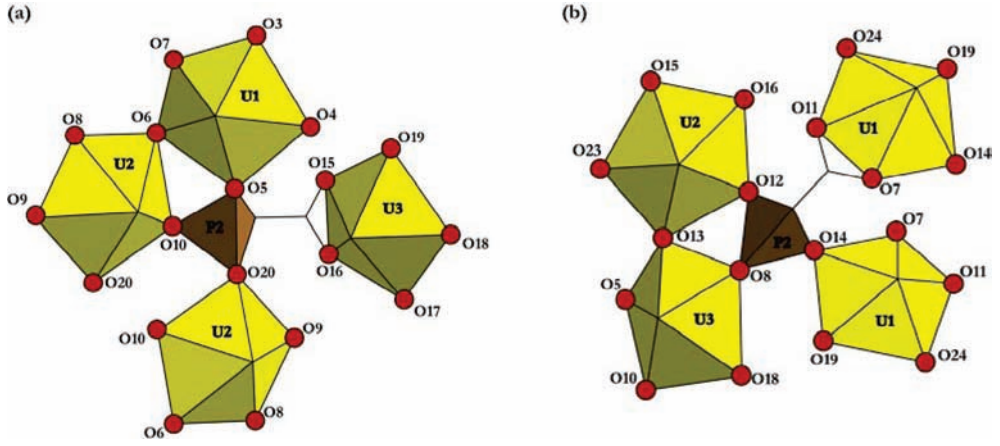

Figure 2. Illustration of the local coordination environment (highlighted in Figure 1) of the phosphonoacetate ligand, P(2)PA, in **1** and **2**. (a) Point shared $(UO_2)_2O_9$ dimers propagate along [001] via coordination of $U(2)O_2^{2+}$ sites to phosphonate oxygen atoms O10 and O20 in **1**. (b) Three crystallographically distinct U(VI) metal centers coordinate to the phosphonate oxygen atoms of P(2)PA in **2**, which thereby links $(UO_2)_2O_9$ dimers with two U(1) monomers.

completed by a phosphonate oxygen O3 from an additional P(3)PA ligand that is also connected to U(2) through both a phosphonate oxygen (O8) and a carboxylate oxygen (O6). Coordination of O6 to both U1 and U2, depicted in Figure 2a, results in point-shared $(UO_2)_2O_9$ dimers. U(2) is additionally bound to two symmetry equivalent P(2)PA units through phosphonate oxygen atoms O(10) and O(20) at distances of 2.349(4) Å and 2.315(4) Å. The coordination sphere of U(2) is completed by a water molecule (O9) that is bound at a U−O distance of 2.467(4) Å. U(3) is equatorially coordinated to three monodentate PPA ligands via phosphonate oxygen atoms O17, O18, and O19. Additionally, a fourth PPA molecule is bound to $U(3)O_2^{2+}$ in a bidentate fashion through carboxylate oxygen atoms O15 and O16.

The $(UO_2)_2O_9$ dimers are linked via two distinct phosphonoacetate molecules, P(2)PA and P(3)PA, to form chains that extend infinitely along [001]. Discrete $U(3)O_2^{2+}$ pentagonal bipyramids are connected by P(1)PA units and likewise propagate along [001]. The two chains are linked along [010] via PPA molecules to result in the two-dimensional (2-D) sheets viewed in Figure 1a. Shown in Figure 3a, the unbound carboxylate oxygen atoms (O21 and O22) of the phosphonoacetate molecule P(1)-PA extend into the interlayer. The $[(UO_2)_3(PPA)_2(HPPA)(H_2O)]^{2-}$ anionic sheets are charge balanced by doubly protonated 4,4′-dipyridyl molecules that are additionally involved in the hydrogen bonding network shown in Figure 3b.

Compound **2**, $[C_{12}H_{12}N_2][(UO_2)_3(PPA)_2(HPPA)(H_2O)]\cdot 2H_2O$, consists of chains of point-shared $(UO_2)_2O_9$ dimers that propagate along [010] via phosphonoacetate molecules. Similarly, pairs of UO_2O_5 monomers connected by phosphonate groups extend down [010]. Linkage of these units along [001] to chains of $(UO_2)_2O_9$ dimers results in the 2-dimensional, anionic sheets shown in Figure 1b. The structure is constructed from three crystallographically distinct UO_2^{2+} sites [U1(O3, O6), U2(O1, O2), and U3(O4, O9)] and three unique phosphonoacetate units. Whereas two of the acid units bind to U(VI) metal centers via both carboxylate and phosphonate moieties, P(1)PA coordinates exclusively through phosphonate oxygen atoms, and the unbound carboxylate groups protrude into the interlayer as illustrated in Figure 4. U(1) is coordinated to four phosphonoacetate

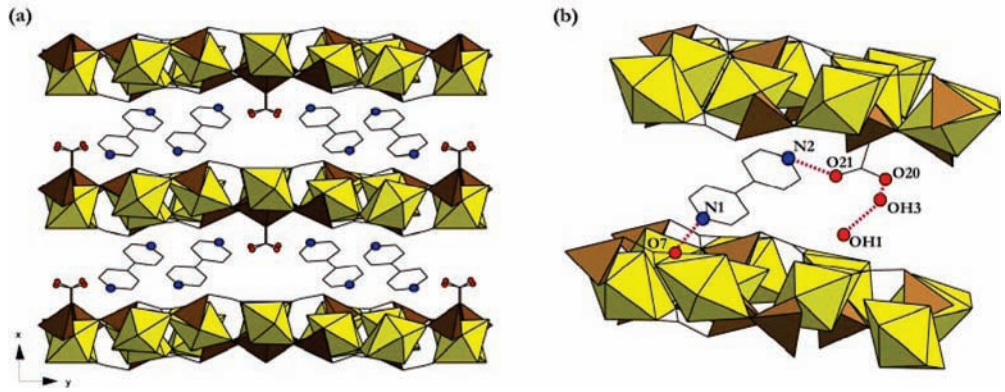

Figure 3. (a) View of **1** down the [001] direction illustrating the stacking of the $[(UO_2)_3(PPA)_2(HPPA)(H_2O)]^{2-}$ sheets along [100]. The unbound carboxylate groups of P(1)PA extend into the interlayer where protonated 4,4′-dipyridyl molecules also reside (b) Illustration of the hydrogen bonding interactions that constitute the interlayer.

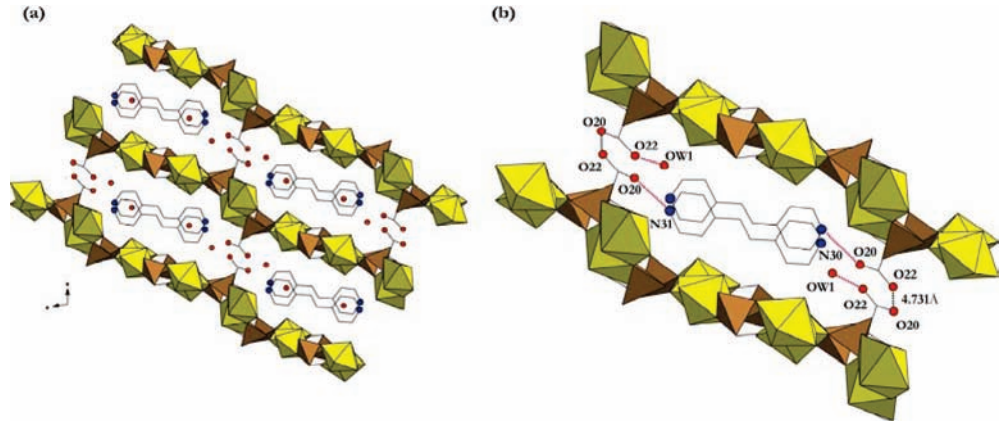

Figure 4. (a) Illustration of **2** down [010] demonstrating the stacking of uranium phosphonoacetate layers. Unbound −COOH moieties protrude into the interlayer where doubly protonated bpe molecules similarly reside. (b) Illustration of the various intermolecular interactions, including the hydrogen bonding network, that form the interlayer.

ligands. Two P(1)PA molecules are coordinated to U(1) through O19 and O24 at distances of 2.264(4) Å and 2.299-(4) Å, respectively, resulting in pairs of $U(1)O_2^{2+}$ monomers. One P(2)PA is bound in a bidentate fashion through carboxylate oxygen atoms O7 and O11 with an average U−O bond distance of 2.504 Å. The coordination environment of U(1) is completed by a phosphonate oxygen O14 from an additional P(2)PA ligand. $U(2)O_2^{2+}$ is equatorially bound to five oxygen atoms from three PPA units and one water molecule. Two of the phosphonoacetate ligands, P(2)PA and P(3)PA, coordinate to the U2 site via phosphonate oxygen atoms O12 and O15 at bond distances of 2.302(4) and 2.319(4) Å. A third PPA is bound in a bidentate manner via carboxylate and phosphonate oxygen atoms O13 and O23 at distances of 2.560(4) Å and 2.319(4) Å, respectively. Finally, U(3) is bound to four phosphonoacetic acid units through phosphonate oxygen atoms O8, O10, and O18 from three PPA molecules (average U−O distance 2.315 Å) and carboxylate oxygen atoms O5 and O13 of an additional PPA ligand (average U−O distance 2.542 Å). Oxygen atom O13 bridges $U(2)O_2^{2+}$ and $U(3)O_2^{2+}$ to form point-shared $(UO_2)_2O_9$ dimers that are linked along [010] to subsequent $(UO_2)_2O_9$ units via P(3)PA molecules as shown in Figure 3. Doubly protonated 1,2-bis(4-pyridyl)-ethylene molecules reside in the interlayer (Figure 4) and charge balance the anionic sheets.

Compound **3**, $[C_{12}H_{14}N_2][(UO_2)_3(PPA)_2(HPPA)(H_2O)]\cdot 2H_2O$ is constructed from $[UO_2)_3(PPA)_2(HPPA)(H_2O)]^{2-}$ sheets that are topologically equivalent to those in **2**. The anionic sheets in **3**, however, are charge balanced by doubly protonated 1,2-bis(4-pyridyl)-ethane molecules that reside in the interlayer.

Fluorescence Studies. The emission spectra for **1** and **3** (Supporting Information, Figures SI 7 and 9) exhibited the characteristic vibronic structure of the UO_2^{2+} cation with five peaks ranging from approximately 470 to 600 nm. Interestingly, **2** exhibits diminished emission (Supporting Information, Figure SI 8) despite its structural similarity to **3**. Lack of emission in **2** is currently under investigation, yet may be attributed to the conjugation of 1,2-bis(4-pyridyl)-ethylene residing in the interlayer. More specifically, the UO_2^{2+} moieties from subsequent layers in **2**, as compared to **3**, are connected by a completely conjugated system because of the —CH=CH— bridge of the 1,2-bis(4-pyridyl)-ethylene molecules. That said, the uranyl cations in **2** are possibly no longer electronically distinct, and quenching is observed as a result.

Thermogravimetric Analysis. Weight loss for **1** occurred in three steps, the first of which (∼2%) took place between approximately 90 and 150 °C and is consistent with the loss of 2 solvent water molecules. A second

weight loss of ~3% occurred between 150 and 250 °C and can be attributed to the loss of the remaining solvent water as well as a bound water molecule. The third step began at 350 °C and was complete by 500 °C. The 15% weight loss observed over this temperature range is attributed to the loss of the 4,4′-dipyridyl and the decomposition of the phosphonoacetate ligand. The total weight loss for **2** was ~17% and occurred in four steps. An initial weight loss of 3% consistent with the loss of lattice water from the structure occurred between 90 and 200 °C. Loss of a bound water molecule subsequently resulted in a ~1% weight loss that was observed between 270 and 300 °C. The third step, attributed to the decomposition of the $-CH_2$ moieties of the phosphonoacetate ligands, occurred shortly thereafter and resulted in a weight loss of an additional 3−4%. A fourth weight loss (~10%) consistent with the decomposition of bpe began at ~350 °C and was complete by ~450 °C. The total weight loss for **3** was 16% and occurred over four steps. Loss of lattice water from the structure began just after 100 °C and was complete by 200 °C. Subsequent loss of the bound water molecule occurred over 250−275 °C. The final weight loss occurred in two steps, beginning around 325 °C and complete by ~550 °C, and can be attributed to the decomposition of bpa and the phosphonoacetate units. TGA plots are available in Supporting Information, Figures SI 10−12.

IR Spectra. Several vibrational modes were observed for compounds **1**−**3** (Supporting Information, Figures SI 13−15). Peaks 3550−3520 cm^{-1} can be attributed to O−H stretching of bound water molecules. The asymmetric and symmetric stretching modes of the UO_2^{2+} cation were observed at 916−908 cm^{-1} and 825−812 cm^{-1}, respectively. The ν(C═O) of the unbound carboxylate moieties are observed at 1680, 1721, 1723 cm^{-1}, whereas the ν(C═O) of the bound carboxylate groups are observed between 1535 and 1500 and 1390−1380 cm^{-1}. The group of peaks around 1000 cm^{-1} corresponds to $-PO_3$ stretches.[49−51]

Discussion

Compounds **1**−**3** are all constructed from $(UO_2)O_5$ pentagonal bipyramids linked via phosphonoacetic acid molecules to form extended 2-D networks. These materials exhibit a variety of structural features and trends consistent with prior accounts of homo- and heterometallic uranium(VI) phosphonoacetate architectures.[7,10] The U(VI) metal centers in **1**−**3**, for example, show an affinity for phosphonate functional groups analogous to that described previously. Albrecht-Schmitt et al. reported a series of UO_2^{2+}/Cu^{2+}/-ppa materials wherein the propensity of the UO_2^{2+} cation to bind preferentially to phosphonate units over carboxylate moieties was used to construct heterometallic UO_2^{2+}/Cu^{2+} carboxyphosphonates.[7] As expected, UO_2^{2+} and Cu^{2+} metal cations showed coordination preferences corresponding to those predicted by Hard/Soft Acid/Base theory.[52] A similar trend was observed in the structure of $(UO_2)(O_3PCH_2CO_2H)$ wherein the harder UO_2^{2+} cation likewise showed preference for the harder $-PO_3^{2-}$ over the softer $-CO_2^-$ moieties, coordinating exclusively to phosphonate oxygen atoms. Compounds **1**−**3** similarly contain a phosphonoacetate unit bound to UO_2^{2+} cations through only phosphonate oxygen atoms, and the unbound carboxylate moieties reside in the interlayer.

Two distinct topologies are observed for the $[(UO_2)_3(PPA)_2(HPPA)(H_2O)]^{2-}$ sheets in the structures of **1**−**3**. Compound **1** consists of rigid 4,4′-dipyridyl molecules whereas **2** and **3** contain more flexible 1,2-bis(4-pyridyl)-ethylene and 1,2-bis(4-pyridyl)-ethane units, respectively. Arguably, slight differences in UO_2^{2+}-PPA coordination modes and hence the topology of the layers in **1** as compared to those in **2** or **3** may, in part, be related to variations in the length and flexibility of 4,4′-dipyridyl as compared to 1,2-bis(4-pyridyl)-ethylene or 1,2-bis(4-pyridyl)-ethane. In addition to serving as charge balancing species, the organic templates in **1**−**3** form interlayer supramolecular networks via the interaction of pyridyl N−H and C−H groups with other functionalities present in the materials. These weak intermolecular interactions characterize the interlayer and likely contribute not only to the stability of the resulting architecture, but also to the overall topology.

Researchers have used weak intermolecular interactions such as hydrogen bonding, halogen bonds, and $\pi-\pi$ interactions within crystal engineering, more generally, to direct the assembly of targeted networks and promote the dimensionality of supramolecular architectures.[53−61] Strong O−H···N interactions between carboxylic acids and pyridine, for example, have been harnessed to co-crystallize a variety of supramolecular structures.[62] Similarly, a combination of O−H···N and O−H···O hydrogen bonding motifs have been used to construct biphosphonic acid-bipyridine base complexes exhibiting 2-D and three-dimensional hydrogen bonding networks.[63] These hydrogen bonding motifs have also been observed in the U(VI)-PPA materials previously reported by our group.[10] Most notably, the interlayer of (UO_2)(HPPA) was dominated by moderately strong head-to-head O−H···O hydrogen bonding interactions (2.658 Å, 161.0°) between unbound carboxylate groups.[10] These acid−acid motifs are absent from the structures of **1**−**3**, and alternatively a combination of strong N−H···O and weaker C−H···O hydrogen bond interactions (Figure 5) are observed.

Interaction of 4,4-dipyridyl with carboxylate, phosphonate and water molecules in **1** results in relatively strong N−H···O hydrogen bonds (2.783−2.815 Å), depicted in Figure 3b, and considerably weaker C−H···O interactions (3.000−3.295 Å) as shown in Figure 5. Intermolecular

(49) Dacheux, N.; Brandel, V.; Genet, M. *New J. Chem.* **1995**, *19*, 15–25.
(50) Dacheux, N.; Brandel, V.; Genet, M. *New J. Chem.* **1995**, *19*, 1029–1036.
(51) Dacheux, N.; Brandel, V.; Genet, M. *New J. Chem.* **1996**, *20*, 301–310.
(52) Pearson, R. G. *J. Chem. Educ.* **1968**, *45*, 581–7.
(53) Etter, M. C. *J. C. Phys. Chem.* **1991**, *95*, 4601–4610.
(54) Desiraju, G. R. *Acc. Chem. Res.* **2002**, *35*, 565–573.
(55) Janiak, C. *Dalton Trans* **2000**, 3885–3896.
(56) Sarkar, M.; Biradha, K. *Cryst. Growth Des.* **2007**, *7*, 1318–1331.
(57) Aakeroy, C. B.; Schultheiss, N. C.; Rajbanshi, A.; Desper, J.; Moore, C. *Cryst. Growth Des.* **2009**, *2009*, 1.
(58) Biradha, K. *CrystEngComm* **2003**, *5*, 374–384.
(59) Metrangolo, P.; Neukirch, H.; Pilati, T.; Resnati, G. *Acc. Chem. Res.* **2005**, *38*, 386–395.
(60) MacGillivray, L. R. *CrystEngComm* **2004**, *6*, 77–78.
(61) Moulton, B.; Zaworotko, M. J. *Chem. Rev.* **2001**, *101*, 1629–1658.
(62) Dale, S. H.; Elsegood, M. R. J.; Hemmings, M.; Wilkinson, A. L. *CrystEngComm* **2004**, *6*, 207–214.
(63) Kong, D.; McBee, J. L.; Clearfield, A. *Cryst. Growth Des.* **2005**, *5*, 643–649.

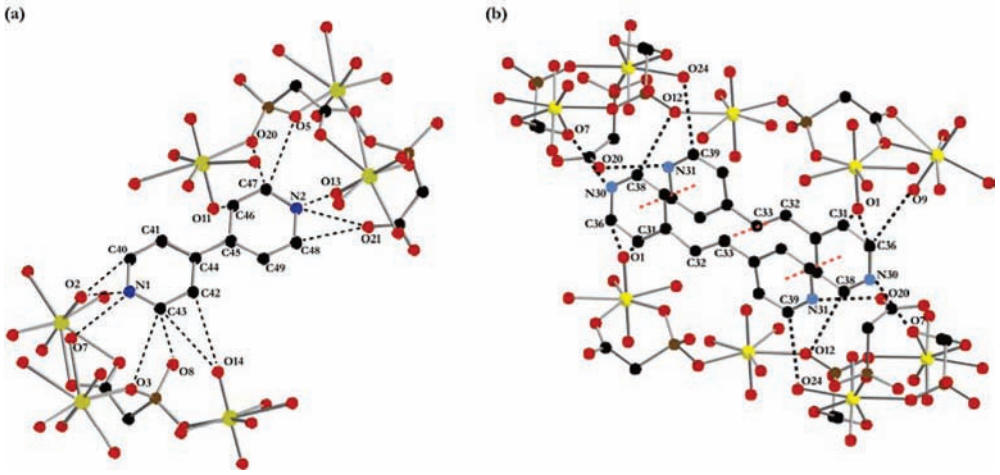

Figure 5. Weak N−H···O and C−H···O hydrogen bonding motifs (black dotted lines) between −NH and −CH groups of (a) 4,4′-dipyridyl or (b) 1,2-bis(4-pyridyl)-ethylene and other functionalities in **1** and **2** respectively. Intermolecular $\pi-\pi$ interactions between pyridyl rings and ethylene bridges in **2** are represented by orange dotted lines. Intermolecular O−H···O hydrogen bonding resulting from lattice water-lattice water and lattice water-carboxylate interactions are not shown.

O−H···O hydrogen bonding (2.663−2.939 Å) resulting from lattice water−lattice water and lattice water−carboxylate interactions are additionally observed in **1**. A combination of noncovalent N−H···O (2.707−3.155 Å), C−H···O (3.087−3.254 Å), and O−H···O (2.669−3.300 Å) interactions are similarly present in the structures of **2** and **3**. Further, the orientation of the pyridyl rings in **2** and **3** suggests that $\pi-\pi$ interactions, interplanar spacing between aromatic groups of approximately 3.3−3.8 Å, are present.[55] Calculated from the center of the pyridyl ring, the centroid−centroid distances in **2** and **3** are 3.708 Å and 3.847 Å, respectively. Moreover, the carbon−carbon double bonds of two 1,2-bis(4-pyridyl)-ethylene molecules in **2** are separated by 3.875 Å. Carbon−carbon double (C═C) bonds that lie approximately parallel and separated by <4.2 Å have been shown to undergo [2 + 2] photodimerization,[64,65] and thus related studies of **2** are currently being explored.

Conclusion

In conclusion, three new templated uranium(VI) carboxyphosphonates have been hydrothermally synthesized and structurally characterized. Despite containing functionally related bipyridyl templates and hence similar O−H···O, N−H···O hydrogen bonding and C−H···O interactions, the architectures, and the interlayer in particular, are distinct. Structural disparity between these materials is largely attributed to differences between the organic dipyridyls (length, flexibility) and is consistent with previous accounts of U(VI) phosphonoacetates wherein the addition of spectator species, the incorporation of charge balancing countercations, and hydrogen bonding networks were found to influence product formation. The fluorescent properties and thermal behavior of these materials was explored. Lack of emission in **2** is likely attributed to additional conjugation (−C═C−) of the 1,2-bis(4-pyridyl)-ethylene, as compared to 1,2-bis(4-pyridyl)-ethane. Further, a preliminary structure refinement suggests that the carbon−carbon double bonds of the 1,2-bis-(4-pyridyl)-ethylene in **2** undergo a partial [2 + 2] photodimerization in the solid state upon prolonged exposure to hν. A detailed study to optimize this transition and explore the resulting structure is under investigation.

Acknowledgment. This work was supported by (1) the National Science Foundation (DMR-0348982 and DMR-0419754), (2) the Chemical Sciences, Geosciences and Biosciences Division, Office of Basic Energy Sciences, Office of Science, Heavy Elements Program, U.S. Department of Energy, under Grant DE-FG02-05ER15736 at GWU, and (3) the ARCS (Achievement Reward for College Scientists) Foundation, Metropolitan Washington tuition reward to K.E.K.

Supporting Information Available: Additional information as noted in the text. This material is available free of charge via the Internet at http://pubs.acs.org.

(64) Schmidt, G. M. J. *Pure Appl. Chem.* **1971**, *27*, 647–678.
(65) MacGillivray, L. R.; Papaefstathiou, G. S.; Friscic, T.; Hamilton, T. D.; Bucar, D.-K. i.; Chu, Q.; Varshney, D. B.; Georgiev, I. G. *Acc. Chem. Res.* **2008**, *41*, 280–291.